Suppression of ionization of heteronuclear diatomic molecules probed by intense lasers

Xianghe Ren[1,2,*] and Takashi Nakajima[2,†]

[1]*College of Sciences, Shandong Polytechnic University, Jinan 250353, China*

[2]*Institute of Advanced Energy, Kyoto University, Gokasho, Uji, Kyoto 611-0011, Japan*

(Received 2 December 2011; published 13 February 2012)

We theoretically investigate the ionization suppression of heteronuclear diatomic molecules and choose NO and NH as examples. These molecules have antibonding molecular orbitals, and hence we expect that the dynamics can be different from those, such as CO, with bonding molecular orbitals we have studied before [Ren and Nakajima, Phys. Rev. A **82**, 063410 (2010)]. Calculations are performed within the framework of strong-field approximation. We find that NO generally exhibits a double-core feature at any laser intensity and hence the ionization suppression is significant. However, it is not as significant as that of O_2 because the interference between the two electron wave packets arising from the N and O cores upon photoelectron ejection cannot be as strong as that of O_2 due to the fact that NO is a heteronuclear diatomic molecule. In contrast, NH exhibits a single-core feature at any laser intensity, since the dominant contribution to ionization comes from the low-energy photoelectron ejections which mainly take place from the neighborhood of the N core. These behaviors of NO (always double-core feature) and NH (always single-core feature) are quite different from that of CO whose ionization behavior gradually changes from the single- to double-core features as the laser intensity increases.

DOI: 10.1103/PhysRevA.85.023403 PACS number(s): 33.80.Rv, 32.80.Rm, 34.50.Gb, 42.50.Hz

I. INTRODUCTION

The interaction of strong laser fields with atoms and molecules results in many different phenomena such as above-threshold ionization (ATI), high-harmonic generation (HHG), and nonsequential double ionization [1–4], etc. Compared with atoms whose ionization dynamics in a strong laser field are essentially determined by their binding energies and the laser parameters, molecules have additional properties to be considered such as the orbital symmetry, orientation of the molecules with respect to the laser field polarization, and interference of electron wave packets from the cores, which may significantly alter the photoionization dynamics [5,6].

Earlier studies showed that the total ionization rates of some diatomic molecules in intense laser fields are nearly equal to those of reference atoms if they have similar ionization potentials [7–9], while recent studies show that this is not always true [10]. For example, it is found that the total ionization rate of N_2 remains comparable to that of the reference atom, Ar, while the total ionization rate of O_2 is much lower than that of the reference atom, Xe. This phenomenon is termed *ionization suppression* and results from the destructive interference of electron wave packets from the two O cores. Motivated by these experimental and theoretical findings, many studies for ionization suppression of molecules have been performed for homonuclear diatomic molecules such as N_2, O_2, D_2, and Cl_2 at the laser wavelength of 0.8 μm [6,11–13]. When we turn to the heteronuclear diatomic molecules, however, there are only a few studies on the ionization suppression. In our recent paper [14], we have investigated strong-field ionization of CO which has a bonding molecular orbital, σ_g, and compared the ionization dynamics with those of N_2 which has the same orbital symmetry. We have found that CO shows a double-core feature (and hence interference effects) only at higher laser intensities, while at low intensities it exhibits a single-core feature (and hence almost no interference). In contrast N_2 always exhibits a double-core feature since it is a homonuclear diatomic molecule. A natural question occurs: How do the heteronuclear diatomic molecules with a different orbital symmetry, i.e., antibonding molecular orbital, behave in the strong laser field?

In this paper we carry out a more comprehensive study on the ionization suppression of heteronuclear diatomic molecules which have antibonding molecular orbitals such as NO and NH, and compare their behaviors with that of CO which has a bonding molecular orbital. The theoretical tool we employ is strong-field approximation (SFA). The reason why we have chosen two different molecules, NO and NH, as examples arises from our speculation that, although both molecules have antibonding molecular orbitals, their response to the strong field may be different, since the physical sizes of N and O are rather similar, while those of N and H are quite different. In Table I we summarize the various properties of molecules and reference atoms we investigate in this paper.

II. IONIZATION-RATE FORMULA

To theoretically study the photoionization processes of atoms and molecules in intense laser fields, the SFA is widely used [15–17]. In this treatment, the Coulomb interaction between the electron and the core can be neglected compared with the electromagnetic interaction between the electron and laser field, and the state of the electron in the intense laser field is described by the Volkov state [18]. Within the SFA, the ionization-rate formula of photoelectrons with a fixed kinetic energy in strong laser field is given by [6,17,19] (the units $c = \hbar = 1$ are used throughout this paper)

$$\frac{dW}{d\Omega_{\mathbf{P}_f}} = \frac{\left(2m_e^3\omega^5\right)^{1/2}}{(2\pi)^2} \sum_{n=n_0}^{N} (n-u_p)^2 (n-u_p-\varepsilon_b)^{1/2} \times |\mathcal{X}_n(Z,\eta)|^2 |\Phi(\mathbf{P}_f,\mathbf{R})|^2, \quad (1)$$

*rxhe@siom.ac.cn

†t-nakajima@iae.kyoto-u.ac.jp

TABLE I. List of the orbital symmetry and ionization potential of molecules and their reference atoms studied in this paper.

Molecules	Orbitals	I_p (eV)	Atoms	I_p (eV)
CO	Bonding (σ_g)	14.01	Kr	14.0
N_2	Bonding (σ_g)	15.58	Ar	15.75
NO	Antibonding (π_g)	9.26	Be	9.32
NH	Antibonding (σ_u)	13.50	Kr	14.0
O_2	Antibonding (π_g)	12.70	Xe	12.13

where $d\Omega_{\mathbf{P}_f} = \sin\theta_f\, d\theta_f\, d\phi_f$ is a differential solid angle of the photoelectron momentum, $\mathbf{P}_f$, and θ_f and ϕ_f are the polar and azimuthal angles of the outgoing photoelectron. $\varepsilon_b = E_b/\omega$ is the molecular binding energy in units of photon energy, ω, n is a number of photons absorbed, and $n_0 = [u_p + \varepsilon_b]_{\rm int} + 1$ is the minimum number of photons needed to reach the ionization threshold. $u_p = U_p/\omega$ is the ponderomotive parameter of the laser fields and is defined as

$$u_p = \frac{e^2 I}{2m_e\omega^3}, \tag{2}$$

with I and m_e being the laser intensity and electron mass, respectively. In Eq. (1), we have employed a generalized phased Bessel (GPB) function, $\mathcal{X}_n(Z,\eta)$, which was first introduced in Ref. [20] and used in Refs. [21–24]. The GPB function introduced in Eq. (1) is defined as

$$\mathcal{X}_n(Z,\eta) = \sum_{k=-\infty}^{+\infty} X_{n-2k}(Z)X_k(\eta), \tag{3}$$

where

$$X_n(Z) = J_n(r)e^{in\varphi} \quad \text{with} \quad Z = re^{i\varphi}, \tag{4}$$

in which $J_n(r)$ is an ordinary Bessel function of order n. The arguments Z and η in Eq. (3) are defined as

$$Z = \frac{e\sqrt{2I}}{m_e\omega^2}\varepsilon\cdot\mathbf{P}_f, \quad \eta = -\frac{1}{2}u_p\cos\xi, \tag{5}$$

where ε is a polarization vector of the laser field and ξ denotes the degree of polarization: $\xi = 0$ and $\pi/2$ correspond to linear and circular polarization, respectively.

In Eq. (1), $\Phi(\mathbf{P}_f,\mathbf{R})$ is the Fourier transformation of the ground-state wave function of the molecule and is rewritten as [16]

$$\Phi(\mathbf{P}_f,\mathbf{R}) = \int d\mathbf{r}\, e^{-i\mathbf{P}_f\cdot\mathbf{r}}\Phi_i(\mathbf{r},\mathbf{R}), \tag{6}$$

where $\Phi_i(\mathbf{r},\mathbf{R})$ is the ground-state wave function of the molecule and $|\mathbf{R}|$ is the internuclear distance. The ground-state wave functions of CO, NO, and NH we will study in this paper are obtained by the Hartree-Fock-Roothaan method [25], and are represented by the linear combination of the Slater-type orbitals, which have the following forms [26]:

$$\phi^{(1s)} = \left(\frac{(Z_h^{(1s)})^3}{\pi}\right)^{1/2}\exp\left(-Z_h^{(1s)}r_h\right),$$
$$\phi^{(2s*)} = \left(\frac{(Z_h^{(2s)})^5}{3\pi}\right)^{1/2} r_h\exp\left(-Z_h^{(2s)}r_h\right),$$

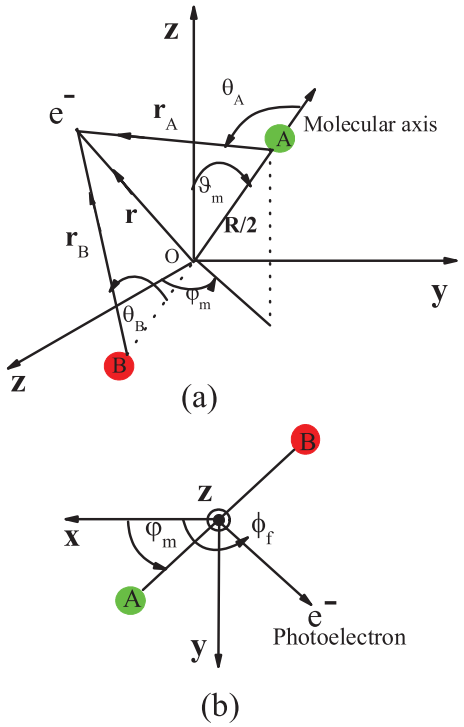

FIG. 1. (Color online) (a) Coordinate system for heteronuclear diatomic molecules (AB) in the ground state without a laser field. (b) Coordinate system for heteronuclear diatomic molecules (AB) upon photoelectron ejection, where ϑ_m has been chosen to be $\pi/2$.

$$\left.\begin{matrix}\phi^{(2p\sigma)}\\ \phi^{(2p\pi)}\\ \phi^{(2p\bar{\pi})}\end{matrix}\right\} = \left(\frac{(Z_h^{(2p)})^5}{\pi}\right)^{1/2} r_h\exp\left(-Z_h^{(2p)}r_h\right) \times \begin{cases}\cos\theta_h\\ \sin\theta_h\cos\phi_h\\ \sin\theta_h\sin\phi_h\end{cases}, \tag{7}$$

where h is the A or B core of the heteronuclear diatomic molecules, r_h is a distance between the electron and the h core, and θ_h, ϕ_h are the polar and azimuthal angles of the electron in the polar coordinate with the z axis taken along the molecular axis as shown in Fig. 1.

Because the function $\phi^{(2s*)}$ is nonorthogonal, it is more convenient to transform it to the orthogonal function using the following formula [27]:

$$\phi^{(2s)} = \frac{\phi^{(2s*)} - S\phi^{(1s)}}{\sqrt{1-S^2}}, \tag{8}$$

where S is the overlap integral between $\phi^{(1s)}$ and $\phi^{(2s*)}$.

Within the framework of SFA employed in this paper, the internal structure of the target (atoms or molecules) plays a very minor role during the ionization processes and hence may be neglected. So here we only consider the outmost electrons in the ground state. The ground-state wave function of CO is given in Ref. [14]. Here we only give the ground-state wave function of NO and NH in the following.

The ground-state wave function of NO is written as [28]

$$\Phi_i^{\rm NO} = c_{\rm N}\phi_{\rm N}^{(2p\pi)} + c_{\rm O}\phi_{\rm O}^{(2p\pi)}, \tag{9}$$

TABLE II. List of the coefficients $c_h^{(l)}$ and the orbital exponents $Z_h^{(l)}$ (h = N,H) for NH.

		$l = 1s$	$l = 2s$	$l = 2p\sigma$
N	$c_{\rm N}^{(l)}$	−0.03117	−0.59895	0.63603
	$Z_{\rm N}^{(l)}$	6.70	1.95	1.95
H	$c_{\rm H}^{(l)}$	0.55503		
	$Z_{\rm H}^{(l)}$	1		

where the coefficients c_h (h = N,O) are 0.8781 and −0.6936, respectively. The orbital exponents in Eq. (7) for NO are $Z_{\rm N}^{(2p)} = 1.95$ and $Z_{\rm O}^{(2p)} = 2.275$.

The ground-state wave function of NH is written as [29]

$$\Phi_i^{\rm NH}(\mathbf{r},\mathbf{R}) = \sum_{h={\rm N,H}} \sum_{l=1s,2s,2p\sigma} c_h^{(l)} \phi_h^{(l)}(\mathbf{r}_h), \qquad (10)$$

where h is N or H. The coefficients $c_h^{(l)}$ and the orbital exponents $Z_h^{(l)}$ in Eq. (7) for NH are listed in Table II. The overlap integrals, S, in Eq. (8) for the atomic orbital of N is $S_{\rm N} = 0.2279$.

III. NUMERICAL RESULTS AND DISCUSSION

As for the laser field we assume that it is linearly polarized along the x axis throughout this paper, and it has a wavelength of 0.8 μm unless otherwise mentioned. As for molecules, we assume that the molecular axis **R** is in the xy plane, i.e., $\vartheta_m = \pi/2$ with arbitrary φ_m as shown in Fig. 1(b), and calculate the differential ionization rates of molecules using Eq. (1). We also carry out similar calculations for the reference atoms. Without a loss of generality we can perform the integration of Eq. (1) over the azimuthal angle, ϕ_f, and all possible photoelectron energies with $\theta_f = \pi/2$ to account for ionization arising from the photoelectrons ejected within the xy plane. Unless otherwise mentioned, the results in this section are obtained by averaging the results over all possible molecular orientations φ_m, from 0 to 2π.

A. Ionization suppression of NO and NH

As an extension of our previous study for CO which has a bonding molecular orbital (for more detail, see Ref. [14]), here we turn to the cases of NO and NH which have antibonding molecular orbitals, and compare their behaviors with that of O_2 which also has an antibonding molecular orbital. The valence electrons of NO are almost equally distributed around both N and O cores, as shown in Fig. 2, and we expect that its behavior would be similar to that of O_2, while those of NH are mostly concentrated around the N core only, as we see in Fig. 3. Therefore, although both NO and NH have the antibonding molecular orbitals, their ionization dynamics will be different.

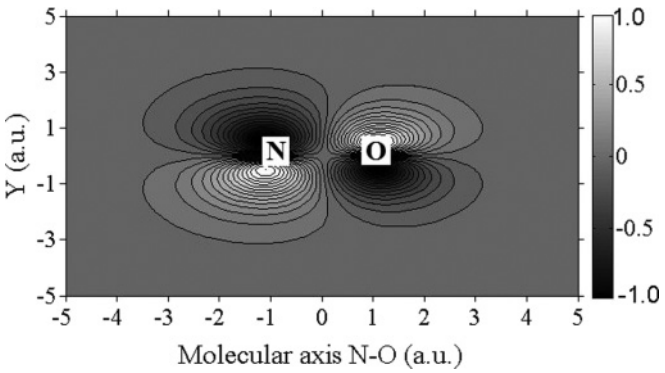

FIG. 2. Valence electron distribution of the NO molecule in the coordinate space.

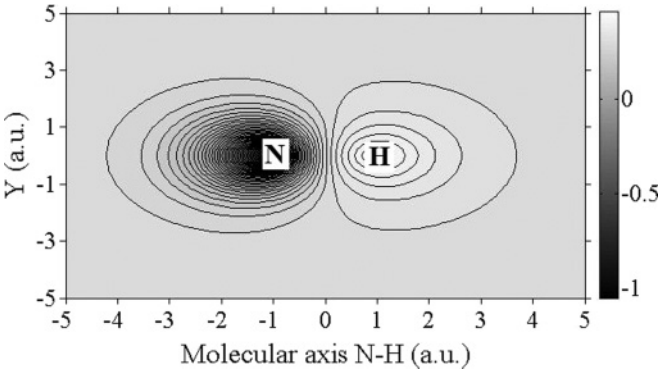

FIG. 3. Valence electron distribution of the NH molecule in the coordinate space.

In Fig. 4 we show the ratios of the total ionization rates of NO versus Be, i.e., NO^+:Be^+, and O_2 versus Xe, i.e., O_2^+:Xe^+, as a function of laser intensity. We see that the ionization suppression of O_2 is always significant over the wide range of laser intensities, although the value of O_2^+:Xe^+ itself becomes larger as the laser intensity increases. The explanation of this result for O_2 is similar to that of CO [14] except for the fact that O_2 is an antibonding orbital molecule and hence the interference term is represented by a sine function, $\sin(\mathbf{P}_f \cdot \mathbf{R}/2)$ [6], instead of a cosine function, $\cos(\mathbf{P}_f \cdot \mathbf{R}/2)$: If the laser intensity is low the dominant contribution to ionization comes from the low-energy photoelectron ejection, and hence $\sin(\mathbf{P}_f \cdot \mathbf{R}/2) \ll 1$. This means that the ionization suppression is significant at low intensities. As the laser intensity increases there is additional contribution to ionization from the high-energy photoelectron ejection, which means

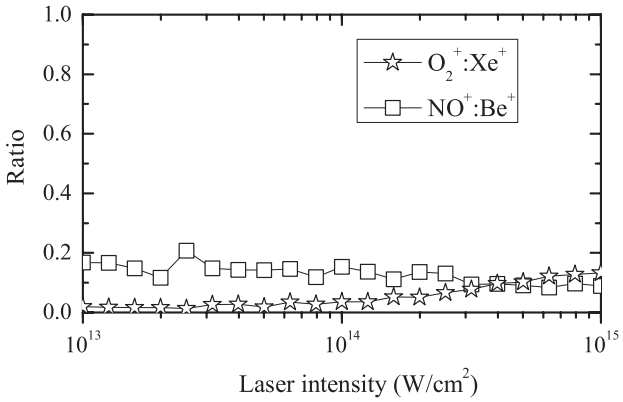

FIG. 4. Ratios of the total ionization rates of NO and O_2 as a function of laser intensity. Molecules are assumed to be randomly oriented in the xy plane.

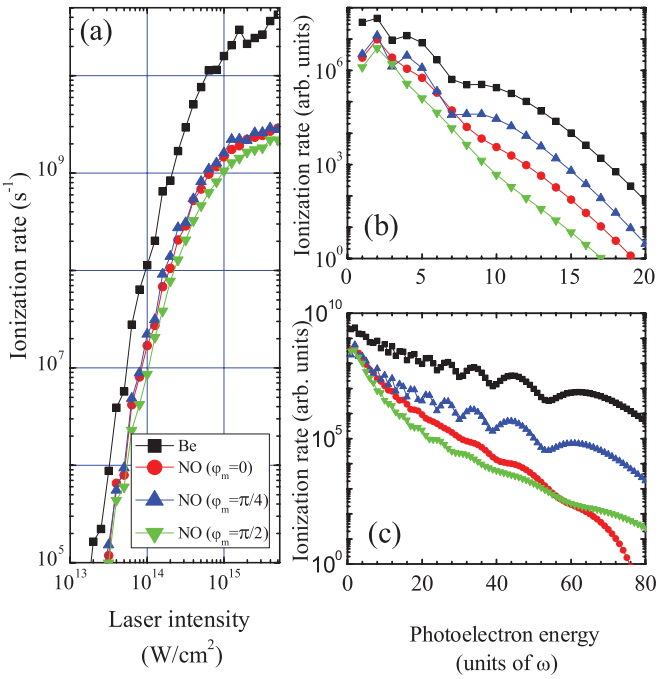

FIG. 5. (Color online) (a) Total ionization rates of NO and Be with different molecular orientations as a function of laser intensity. Photoelectron energy spectra of NO and Be for different molecular orientations at the laser intensities of (b) 10^{14} and (c) 10^{15} W/cm^2. $\varphi_m = 0$ means that the molecule is oriented along the direction of laser polarization.

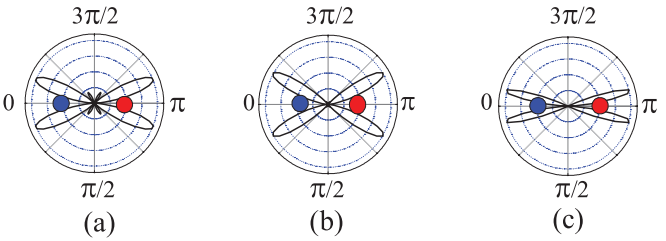

FIG. 6. (Color online) PADs of NO for three different photoelectron energies at the laser intensity of 10^{14} W/cm^2. The photoelectron energies are (a) 0.26, (b) 1.76, and (c) 18.25 eV, respectively. NO is assumed to be oriented along the x axis; that is, $\vartheta_m = \pi/2$ and φ_m=0, where the N and O cores are described by the circles filled with blue (left) and red (right), respectively.

that $\sin(\mathbf{P}_f \cdot \mathbf{R}/2) < 1$, and hence the ionization suppression becomes less significant, i.e., the value of O_2^+:Xe^+ becomes larger but still far smaller than unity.

As for NO, it has an antibonding molecular orbital similar to O_2. From Fig. 4, we find that the ionization suppression of NO is also very significant over the wide laser intensity range from 10^{13} to 10^{15} W/cm^2. The value of NO^+:Be^+, however, is around 0.1–0.2, which is larger than that of O_2^+:Xe^+. Only if the laser intensity is above 4×10^{14} W/cm^2 does the value of NO^+:Be^+ become similar to that of O_2^+:Xe^+. This is somehow expected, since the valence electron distribution of NO is almost equally distributed around both N and O cores, as we have seen in Fig. 2, which implies that NO would have a double-core feature irrespective of the laser intensity. This explains why the ionization suppression (interference effect) of NO is significant at any laser intensity. However, the interference effect of NO is not as strong as that of O_2, since the former is a heteronuclear diatomic molecule. As the intensity increases, the interference becomes stronger, since the rate of photoelectron ejection from the neighborhood of the O core becomes larger and comparable to that from the N core. Recall that the O core has a bit higher electronegativity than the N core. We point out that the above argument to explain the intensity-dependent ionization suppression of NO is similar to that for CO [14].

Figure 5(a) shows the total ionization rates of NO with different molecular orientations as a function of laser intensity. For comparison the total ionization rate of Be is also shown. It is clear that the total ionization rate of NO depends on the molecular orientation, and moreover, the ionization suppression is significant at any molecular orientation. We also notice that the total ionization rate of NO takes the largest value at $\varphi_m = \pi/4$. This is because the valence electrons of NO approximately locate along the two diagonals in the xy plane like a butterfly, as shown in Fig. 2. The photoelectron energy spectra of NO also depend on the molecular orientation, as shown in Figs. 5(b) and 5(c) for 10^{14} and 10^{15} W/cm^2, respectively. Compared with Be the photoelectron energy spectra of NO at different molecular orientations are very much suppressed due to the destructive interference effect. For NO with $\varphi_m = \pi/2$, the overall photoelectron energy spectrum is located lower than those with $\varphi_m = 0$ and $\pi/4$. This is because the nodal plane of NO in terms of valence electron distribution is perpendicular to the molecular axis, as we see in Fig. 2.

Figure 6 presents the photoelectron angular distributions (PADs) of NO for three different photoelectron energies at the laser intensity of 10^{14} W/cm^2. Generally speaking, the PADs of NO are nearly fourfold symmetric about the molecular axis and its vertical axis at any photoelectron energy. There is no photoelectron ejection parallel and perpendicular to the molecular axis simply because there are two nodal planes for the valence electron distribution, as we see in Fig. 2. Figure 6 also confirms that NO generally shows a double-core feature at any photoelectron energy.

NH also has an antibonding molecular orbital. But its electronic state is in the σ_u symmetry. As we have seen in Fig. 3 the valence electrons of NH are mostly concentrated around the N core and along the molecular axis, which is quite different from that of NO and O_2. In this sense the valence electron distribution of NH is rather similar to that of CO. There is, however, an important difference. There is a nodal plane in NH (Fig. 3), while it is absent for CO (Fig. 2 of Ref. [14]). Therefore we can expect that the ionization dynamics of NH in strong laser fields may show some new interesting features which may be different from those of NO and CO.

Figure 7 presents the ratio of the total ionization rates of NH and Kr as a function of laser intensity. Although NH has an antibonding orbital, the ratio of NH^+:Kr^+ is around 0.6, which is larger than that of NO^+:Be^+ and O_2^+:Xe^+, indicating that the ionization suppression of NH is not as significant as that of NO and O_2. This is somehow expected, since the valence electrons of NH are mostly distributed in the neighborhood of the N core. That is, NH shows a single-core feature, which is similar to the case of CO. Examination of PADs can shed more

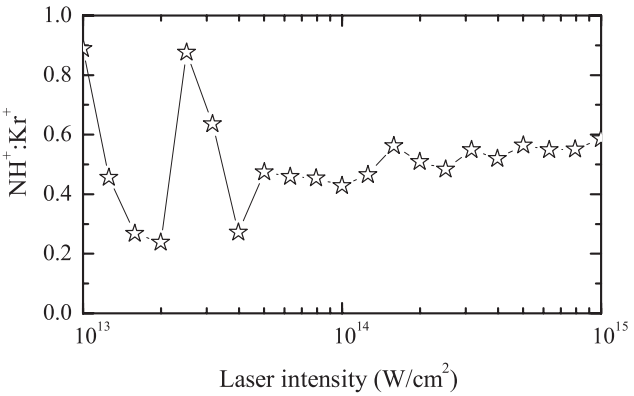

FIG. 7. Ratio of the total ionization rates of NH and Kr as a function of laser intensity. Molecules are assumed to be randomly oriented in the xy plane.

light on the similarity as well as the difference between NH and CO. In Fig. 8, we present the PADs of NH for three different photoelectron energies at the laser intensity of 10^{14} W/cm^2. At the photoelectron energy of 0.96 eV, the photoelectrons ejection mainly takes place from the neighborhood of the N core and the PAD is not inversion symmetric, which is similar to CO. However, this single-core feature of NH remains even for higher photoelectron energies as we see in Figs. 8(b) and 8(c), while the single-core feature of CO gradually disappears as the photoelectron energy increases (Figs. 5(b) and 5(c) of Ref. [14]). In other words, NH has a stronger single-core feature than CO.

Orientation dependence of the ionization rate of NH further reveals the difference between NH and CO. Recall that, although both CO and NH have a single-core feature rather than a double-core feature at low laser intensities, their valence electron distributions are quite different as we have seen in Fig. 3 of Ref. [14] and Fig. 3. The most important difference is that the valence electron distribution of NH has a nodal plane. This explains why the ionization rate of NH is so small at $\varphi_m = \pi/2$ [Fig. 9(a)], regardless of the laser intensities [Figs. 9(b) and 9(c)]. Note that the orientation dependence of the ionization rate of CO is rather weak, in particular, at the laser intensity below 10^{14} W/cm^2 (Fig. 10(b) of Ref. [14]).

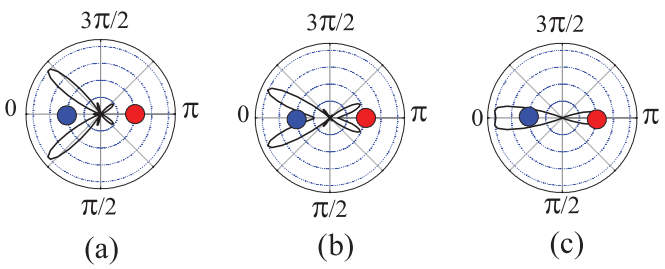

FIG. 8. (Color online) PADs of NH for three different photoelectron energies at the laser intensity of 10^{14} W/cm^2. The photoelectron energies are (a) 0.96, (b) 2.52, and (c) 14.91 eV, respectively. NH is assumed to be oriented along the x axis, that is, $\vartheta_m = \pi/2$ and $\varphi_m = 0$, where the N and H cores are described by the circles filled with blue (left) and red (right), respectively.

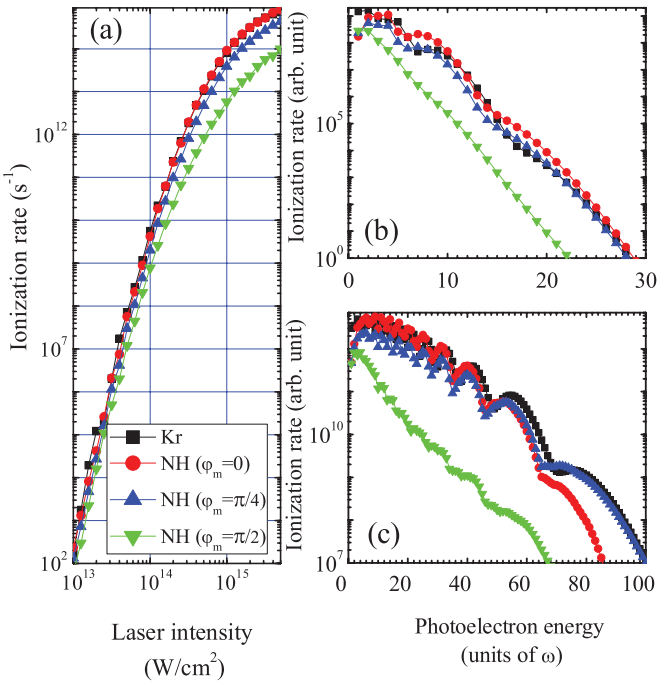

FIG. 9. (Color online) (a) Total ionization rates of NH and Kr with different molecular orientations as a function of laser intensity. Photoelectron energy spectra of NH and Kr for different molecular orientations at the laser intensities of (b) 10^{14} and (c) 10^{15} W/cm^2. $\varphi_m = 0$ means the molecule is oriented along the direction of laser polarization.

B. Wavelength dependence of ionization suppression

In earlier works [6,10,11,14,19] about ionization suppression the Ti:sapphire laser wavelength, 0.8 μm, has been employed. In this section we consider the wavelength dependence of ionization suppression. Figure 10 shows the variation of the ratios of ionization rates of N_2 and CO compared with their reference atoms, Ar and Kr, i.e., N_2^+:Ar^+ and CO^+:Kr^+, as a function of laser intensity for three different laser wavelengths.

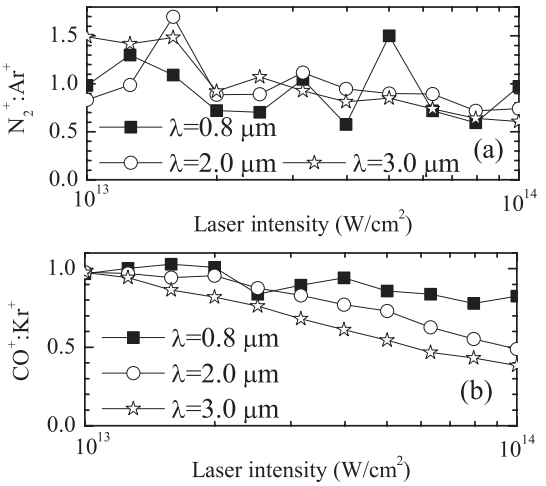

FIG. 10. Ratios of the total ionization rates of (a) N_2 versus Ar and (b) CO versus Kr as a function of laser intensity for three laser wavelengths: 0.8, 2.0, and 3.0 μm. Molecules are assumed to be randomly oriented in the xy plane.

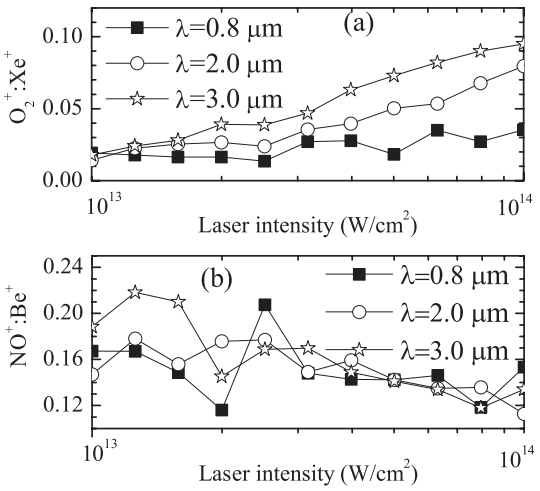

FIG. 11. Ratios of the total ionization rates of (a) O_2 versus Xe and (b) NO versus Be as a function of laser intensity for three laser wavelengths, 0.8, 2.0, and 3.0 μm. Molecules are assumed to be randomly oriented in the xy plane.

From Fig. 10(a) we can see that the ionization suppression of N_2 has no obvious wavelength dependence in this intensity range. In contrast, as shown in Fig. 10(b), the ionization suppression of CO appears to become more significant for the longer laser wavelength. In order to understand this tendency we recall that, as we have clarified in Ref. [14], CO shows a double-core feature only if the photoelectron ejection from the neighborhood of the O core becomes comparable to that from the neighborhood of the C core, and this will take place if the photoelectron energy is large. Moreover, provided with the fixed laser intensity, strong-field ionization by the laser with a longer laser wavelength results in the production of photoelectrons with higher energy due to the larger ponderomotive energy. The above arguments explain why the ionization suppression is more significant for the longer laser wavelength under the same laser intensity.

Figure 11 shows similar results for O_2 and NO. The wavelength and intensity dependence shown in Fig. 11(a) can be easily explained from the arguments we have made in Sec. III A in terms of the interference term, $\sin(\mathbf{P}_f \cdot \mathbf{R}/2)$. For the longer laser wavelength the photoelectron momentum $\mathbf{P}_f$ becomes larger at the same laser intensity, and hence the ionization suppression becomes less significant at the longer laser wavelength. As for NO, Fig. 11(b) shows that there is no obvious wavelength dependence, which is quite different from the case of CO, and it is because NO has a double-core feature at any laser intensity and any laser wavelength. Therefore we cannot make a simple argument as in the case of CO to explain the results for NO.

IV. CONCLUSIONS

In conclusion, we have theoretically studied the ionization suppression of heteronuclear diatomic molecules through the comparisons of valence electron distributions, total ionization rates, photoelectron angular distributions, and photoelectron energy spectra for the NO and NH molecules as examples and compared with those for CO [14]. To briefly summarize the difference and similarity among NO, NH, and CO, we can say the following: NO and NH have the antibonding molecular orbitals and their valence electron distributions show the nodal planes. The essential difference between NO and NH in terms of strong-field ionization comes from the fact that NO shows a strong double-core feature at any laser intensity since the photoelectron ejection takes place from the neighborhood of both N and O cores at any photoelectron energy and laser intensity, as we can expect from its valence electron distributions (Fig. 2). In contrast NH shows a single-core feature as we can imagine from Fig. 3 and most of ionization takes place from the neighborhood of the N core, and accordingly the ionization suppression of NH is less significant compared with NO. In this sense NH is similar to CO which also shows a single-core feature at low laser intensities [14]. There is, however, a big difference between them. The valence electron distribution of NH has a nodal plane which is absent for CO, and this explains why the orientation dependence of the ionization rate and hence the ionization suppression of NH is seen at any laser intensity, if the ionization rate is averaged over all molecular orientations.

ACKNOWLEDGMENTS

T.N. acknowledges useful discussions with Prof. Yukiyoshi Ohtsuki and Dr. Ryuji Itakura. The work by X.H.R. and T.N. was, respectively, supported by the National Science Foundation of China under Grant No. 11104167, Excellent Middle-Aged and Youth Scientist Award Foundation of Shandong Province of China (Grant No. BS2011SF021), and the Grant-in-Aid for scientific research from the Ministry of Education and Science of Japan.

[1] P. B. Corkum, Phys. Rev. Lett. **71**, 1994 (1993).
[2] P. Agostini, F. Fabre, G. Mainfray, G. Petite, and N. K. Rahman, Phys. Rev. Lett. **42**, 1127 (1979).
[3] L. Pei and C. Guo, Phys. Rev. A **82**, 021401(R) (2010).
[4] Y. M. Zhou, Q. Liao, Q. B. Zhang, W. Y. Hong, and P. X. Lu, Opt. Exp. **18**, 632 (2010).
[5] D. Pavićić, K. F. Lee, D. M. Rayner, P. B. Corkum, and D. M. Villeneuve, Phys. Rev. Lett. **98**, 243001 (2007).
[6] X. H. Ren, J. T. Zhang, P. Liu, Y. Wang, and Z. Z. Xu, Phys. Rev. A **78**, 043411 (2008).
[7] G. N. Gibson, R. R. Freeman, and T. J. McIlrath, Phys. Rev. Lett. **67**, 1230 (1991).
[8] S. L. Chin, Y. Liang, J. E. Decker, F. A. Ilkov, and M. V. Ammosov, J. Phys. B **25**, L249 (1992).
[9] T. D. G. Walsh, F. A. Ilkov, J. E. Decker, and S. L. Chin, J. Phys. B **27**, 3767 (1994).
[10] C. Guo, M. Li, J. P. Nibarger, and G. N. Gibson, Phys. Rev. A **58**, R4271 (1998).
[11] J. Muth-Böhm, A. Becker, and F. H. M. Faisal, Phys. Rev. Lett. **85**, 2280 (2000).

[12] A. Talebpour, S. Larochelle, and S. L. Chin, J. Phys. B **31**, L49 (1998).
[13] E. P. Benis, J. F. Xia, X. M. Tong, M. Faheem, M. Zamkov, B. Shan, P. Richard, and Z. Chang, Phys. Rev. A **70**, 025401 (2004).
[14] X. H. Ren and T. Nakajima, Phys. Rev. A **82**, 063410 (2010).
[15] D. B. Milošević, Phys. Rev. A **74**, 063404 (2006).
[16] H. R. Reiss, Phys. Rev. A **22**, 1786 (1980).
[17] A. Becker and F. H. M. Faisal, J. Phys. B **38**, R1 (2005).
[18] D. M. Volkov, Z. Phys. **94**, 250 (1935).
[19] A. Jaroń-Becker, A. Becker, and F. H. M. Faisal, Phys. Rev. A **69**, 023410 (2004).
[20] D.-S. Guo, R. R. Freeman, L. Gao, X. Li, P. Fu, T. Edis, and A. Troha, J. Phys. B **34**, 2983 (2001).
[21] J. T. Zhang, W. Q. Zhang, Z. Z. Xu, X. F. Li, P. M. Fu, D.-S. Guo, and R. R. Freeman, J. Phys. B **35**, 4809 (2002).
[22] J. T. Zhang and Z. Z. Xu, Phys. Rev. A **68**, 013402 (2003).
[23] L. H. Bai, J. T. Zhang, Z. Z. Xu, and D.-S. Guo, Phys. Rev. Lett. **97**, 193002 (2006).
[24] J. T. Zhang and T. Nakajima, Phys. Rev. A **75**, 043403 (2007).
[25] C. C. J. Roothann, Revs. Mod. Phys. **23**, 69 (1951).
[26] J. Slater, Phys. Rev. **36**, 57 (1930).
[27] H. Brion and C. Moser, J. Chem. Phys. **32**, 1194 (1960).
[28] H. Rrion and M. Yamazaki, J. Chem. Phys. **30**, 673 (1959).
[29] J. Higuchi, J. Chem. Phys. **24**, 535 (1956); M. E. Boyd, *ibid.* **29**, 108 (1958).